72º Congresso Anual da ABM
Anais do Congresso Anual da ABM ISSN 2594-5327 vol. 72, num. 1 (2017)

TECHNOLOGIES OF ALUMINA-MAGNESIA REFRACTORIES FOR STEEL LADLES PART II, CASTABLE PROPERTIES UNDER RESTRAINED HEATING*

Kazuya Nakabo[1]
Shigefumi Nishida[2]
Masatsugu Kitamura[3]

Abstract

In this article, influences of restraint and MgO content on densification of alumina-magnesia castable during heating were experimentally studied. High thermal expansion-alumina-magnesia castable specimens were surrounded by low thermal expansion-alumina-silica castables, and heated in an electric furnace. Doing so allows restrained heating of alumina-magnesia castable. According to the results of simple calculations, the restraint stresses were estimated to be between 2 to 20 MPa, so the experimental conditions were considered reasonable.

As a result of the experiments, it was verified that restraint densifies alumina-magnesia castable, resulting in an increase in modulus of rupture and modulus of elasticity. The densification effect of restraint became larger as the MgO content increased. The effects are attributable to an in-situ spinel forming reaction, which improves corrosion resistance.

Taking the temperature distribution in the castable lining into account, large restraint stress is expected for the hot face while only a little effect is expected for back end. Thus, excessive difference in material property in the thickness direction, which is undesirable in terms of structural spalling, is a concern.

Hence, the MgO content of alumina-magnesia castable should be determined carefully, taking not only corrosion resistance but also spalling resistance into consideration.

Keywords: Refractories; Castable; Steel ladle; Thermal behavior.

[1] *Master, Osaka City Univ., Assistant Manager, Research Laboratory, Shinagawa Refractories Co., Ltd., Bizen, Okayama Pref. Japan.*
[2] *Master, Konan Univ., Manager, Research Laboratory, Shinagawa Refractories Co., Ltd., Bizen, Okayama Pref. Japan.*
[3] *Bachelor, Hokkaido Univ., General Manager, Research Laboratory, Shinagawa Refractories Co., Ltd., Bizen, Okayama Pref. Japan.*

** Technical contribution to the 72º Congresso Anual da ABM – Internacional e ao 17º ENEMET - Encontro Nacional de Estudantes de Engenharia Metalúrgica, de Materiais e de Minas, part of the ABM Week, October 2nd-6th, 2017, São Paulo, SP, Brazil.*

1 INTRODUCTION

For decades, Japanese integrated steel mills have been adopting castable refractories to the metal line and bottom of steel ladles because of the easy installation procedure without the requirement of skilled masons, as well as formation of jointless monolithic structure. Since the early 1990's, alumina-magnesia castable refractories, which are composed of alumina and magnesia raw materials [1]-[3], have been widely used due to superior corrosion and slag penetration resistance. These favorable properties are attributed to microstructure strengthening induced by an in-situ spinel forming reaction as expressed in Equation 1.

$$Al_2O_3 + MgO \rightarrow Al_2MgO_4 \quad (1)$$

As a result of the reaction, alumina-magnesia materials tend to exhibit large thermal expansion in the temperature range between 1200 ˚C-1400 ˚C under non-restrained conditions, resulting in large permanent linear changes (hereinafter, referred to as PLC).
However, the expansion is limited by the surrounding structural members in actual use. In addition, the materials show creep behavior at high temperature [4]. Therefore, the material texture under restraint is considered to be denser than that under non-restrained conditions. Although experimental heating under load is possible by utilizing apparatus for the thermal creep experiment or the refractoriness under load evaluation, the imposed load is usually 0.2 to 0.5 MPa, which is considered to be much smaller than the actual use restraint load.
Braulio et al. [5] conducted bi-axial restrained heating experiments. They heated large expansion-alumina-magnesia castable specimens surrounded by low thermal expansion-alumina-silica castable. The alumina-magnesia materials were densified by heating under restrained conditions. According to those results, they concluded that the densification improves slag penetration resistance. In their study, the influence of particle size was evaluated.
Kitanaka et al. [6] carried out mono-axial restrained heating experiments in which both ends of the rectangular specimens were fixed. As a result of the experiment, they observed that the specimens were cracked and buckled. Therefore, they concluded that excessive expansion of castables possibly deteriorates spalling resistance. However, mono-axial restraint is considered to be inadequate for reproducing the restraint of an actual steel ladle.
In this study, the authors evaluated the influences of MgO content and bi-axial restraint on castable properties and their effects on spalling resistance are discussed.

2 MATERIAL AND METHODS

2.1 Procedure and mathematical model of restraint heating

Figure 1 schematically shows the specimen shape for restraint heating. High thermal expansion-alumina-magnesia test materials are surrounded by alumina-silica castable that shows lower thermal expansion. Restraint heating of alumina-magnesia test materials is achievable by heating these combined bodies in an electric furnace.

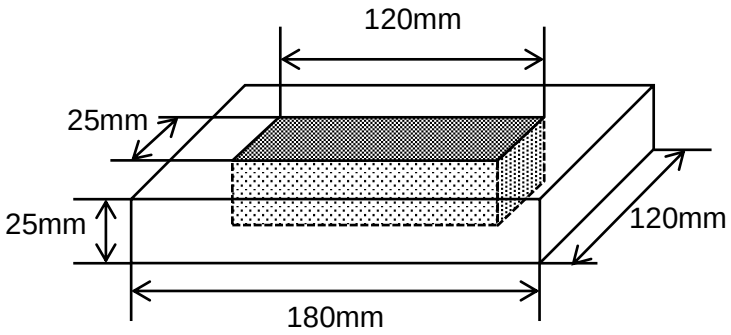

Figure 1. Schemaic diagram of restrained specimen.

Since the surrounding outer castable shows thermal expansion, the inner test materials are not completely restrained. Under these experimental conditions, stress loaded on test materials can be estimated mathematically.
Figure 2 shows a schematic diagram of a mathematical model in which the inner test material and outer castable adhere completely. At elevated temperatures, high thermal expansion-inner test material is shortened and low thermal expansion-outer castable are lengthened from their natural expansion position in order to maintain identical overall expansion. In this situation, compressive stress and tensile stress are applied on the inner test material and outer castable, respectively, according to their elasticities. The overall expansion can be calculated since it is at the position at which the compressive force applied on the inner test material is equivalent to tensile force applied on the outer castable. Thus, stress loaded to specimen can be estimated by thermal expansions, hot modulus of elasticities (hereinafter, referred to as HMOE) and cross sectional areas of each material.

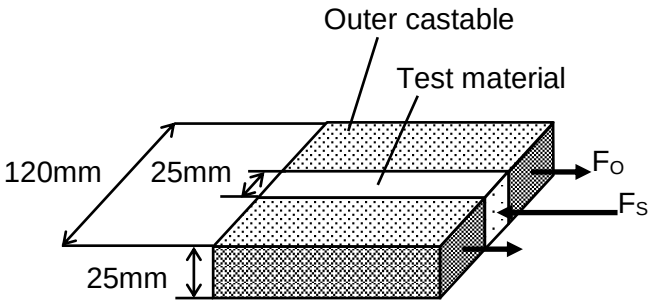

Figure 2. Schematic diagram of model to estimate stress generated by restraint.

In the following mathematical model description, suffixes "$_c$", "$_i$" and "$_o$" indicate combined body, inner test material and outer castable, respectively. Assuming the overall expansion of the combined body, natural coefficients of thermal expansion, HMOEs at elevated temperature (T) and cross sectional areas as $\alpha_c(T)$, $\alpha_i(T)$, $\alpha_o(T)$, $E_i(T)$, $E_o(T)$, S_i and S_o, respectively, forces acting on inner test material and outer castable ($F_i(T)$ and $F_o(T)$) are expressed as Equations 2 and 3, respectively.

$$F_i(T) = \left(\alpha_i(T) - \alpha_C(T)\right) \cdot E_i(T) \cdot S_i \quad (2)$$

$$F_O(T) = \left(\alpha_C(T) - \alpha_O(T)\right) \cdot E_O(T) \cdot S_O \quad (3)$$

According to the assumption, Equation 4 is obvious.

$$F_i(T) = F_O(T) = F(T) \quad (4)$$

By solving simultaneous equations (Equations 2 and 3), F(T) is given by Equation (5).

$$F(T) = \frac{\alpha_i(T) - \alpha_O(T)}{\left(E_i(T)\cdot S_i\right)^{-1} + \left(E_O(T)\cdot S_O\right)^{-1}} \quad (5)$$

Hence, stress loaded to inner test material at temperature T ($\sigma_i(T)$) can be estimated by Equation (6)

$$\sigma_i(T) = \frac{\alpha_i(T) - \alpha_O(T)}{\left\{\left(E_i(T)\cdot S_i\right)^{-1} + \left(E_O(T)\cdot S_O\right)^{-1}\right\}\cdot S_i} \quad (6)$$

Strictly speaking, thermal expansion and restraint occur in three dimensions. In this study, however, a one dimensional mathematical model was employed for convenience sake.

2.2 Specimen preparations

Table 1 provides the characteristics of the materials. Three alumina-magnesia castables containing different amounts of MgO were used as test materials. The outer castable is alumina-silica material which shows good spalling resistance and small PLC.

Table 1. Characteristics of specimens and outer castable

		Test materials (a)	(b)	(c)	Outer castable
Chemical composition / mass%	Al_2O_3	87	91	95	57
	MgO	11	7	3	
	SiO_2	1	1	1	39
Maximum particle size / mm		5	5	5	5
Water content / mass%		5.5	5.5	5.5	6.5

The test materials were mixed with water and mixtures were cast into a 25 mm × 25 mm × 120 mm rectangular mold. The test material filled molds were left on a horizontal table at room temperature over 24 hours for curing. The cured test materials were demolded and put at the center of another 120 mm × 25 mm × 180 mm mold followed by outer castable casting to the surrounding area of the test materials. Subsequent to outer castable curing and demolding, the combined bodies were dried at 110 ˚C for 24 hours.
Additionally, in order to evaluate other properties, which will be described in the next subsection, some other test materials specimens and outer castables were prepared by the same procedure, i.e., casting, curing and drying.

2.3 Property evaluations

The evaluated properties and heating conditions are summarized in Table 2. According to the mathematical model mentioned in subsection 2.1, thermal expansions and HMOEs of test materials and outer castable are necessary for restraint stress estimation. For the estimation, static modulus of elasticity rather than dynamic modulus of elasticity is suitable. Therefore, the HMOE were evaluated by static method. Taking time consuming procedure of static HMOE evaluation and required accuracy of estimation into account, evaluations of static HMOEs were performed just for test material (b) and outer castable.
Properties of test materials after heating with and without restraint at 1000 ˚C, 1300 ˚C and 1500 ˚C were evaluated. In order to verify the influences of restraint, microstructure observation and pore size determination were carried out.
Static HMOEs and modulus of ruptures (hereinafter referred to as MOR) after heating were evaluated by three point bending method. The apparent porosities (hereinafter, referred to as AP) and dynamic MOE after heating were mesured by Archimedes method and Grindosonic method, respectively. The pore size distrubutions were determied by mercury intrusion method. An EPMA was utilized to observe the microstructures of the materials.

Table 2. Materials subjected to evaluations

Evaluations	**Heating conditions**	
	1000 ˚C, 1300 ˚C, 1500 ˚C for 3 hours in air	**1500 ˚C for 3 hours in air**
Thermal expansion at elevated temperatures without restraint	(a), (b), (c), outer castable	-
Static hot modulus of elasticity(static HMOE) at elevated temperatures	(b), outer castable	-
Permanent linear change (PLC) after heating with and without restraint	(a)	(a), (b), (c)
Apparent porosity (AP) after heating with and without restraint	(a)	(a), (b), (c)
Modulus of rupture (MOR) after heating with and without restraint	(a)	(a), (b), (c)
Dynamic modulus of elasticity (MOE) after heating with and without restraint	(a)	(a), (b), (c)
Microstructure observation after heating with and without restraint	-	(b)
Pore-size distribution after heating with and without restraint	-	(b)

3 RESULTS AND DISCUSSION

In this section, evaluated properties will be demonstrated subsequent to description of restraint stress estimation. Then, the cause of property variations and their influences on commercial application will be discussed comprehensively in terms of microstructure evolution.

3.1 Estimation of restraint stress

Figures 3 and 4 show the linear changes of all materials and the HMOEs of (b) and the outer castable at each temperature, respectively. The thermal expansions of test specimens increased as the MgO content increased. The outer castable showed the

lowest thermal expansion. While the HMOE of the test material (b) decreased linearly as temperatures rose, the outer castable showed the highest HMOE at 1300 ˚C.
By using the evaluated values shown in Figures 3 and 4, restraint stresses acting on test materials were estimated according to Equation 6. For calculation, the HMOEs of test materials were assumed to be identical. Figure 5 summarily shows the calculated results. The stress values were calculated between 2 and 20 MPa, which are considered to be reasonable.
According to Figure 5, restraint stress became larger as the MgO content of the test material increased. That is attributable to variation in thermal expansion. The restraint stresses at 1500 ˚C were smaller than those at 1300 ˚C since the HMOEs of the test materials at 1500 ˚C were smaller than those at 1300 ˚C.

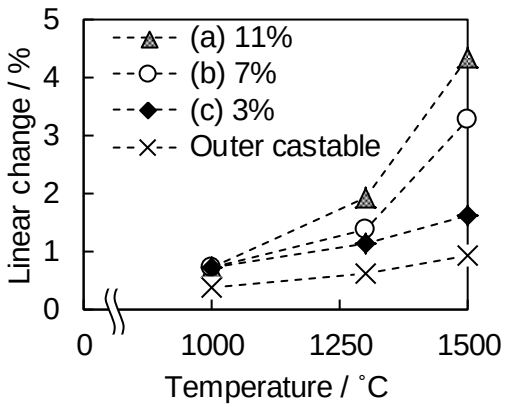

Figure 3. Linear change of test materials and outer caastable at each temperature.

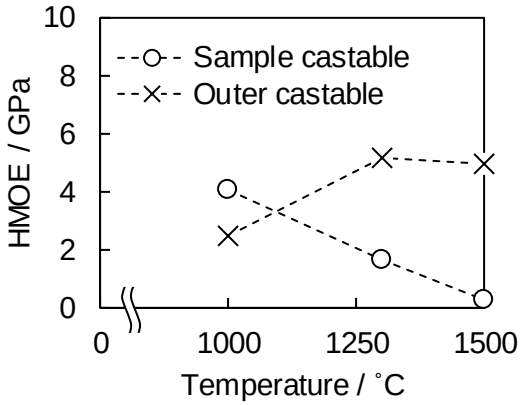

Figure 4. Hot static modulus of elasticity of test material (b) and outer castable.

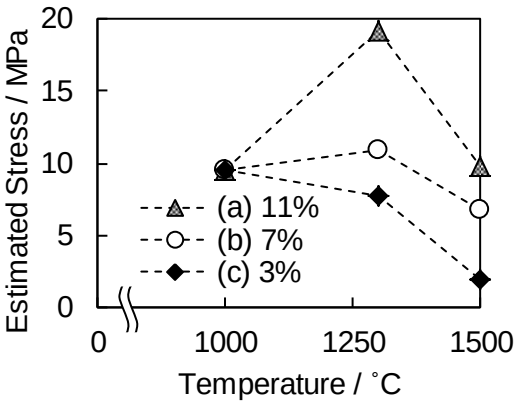

Figure 5. Variations of estimated stress acting on the restrained specimens along longitudinal direction.

3.2 Physical properties and microstructure of test materials after heating with and without restraint

The evaluated properties are shown in Figures 6 to 13. The PLCs of the non-restrained test materials (b) increased in accordance with heating temperature increase. In terms of MgO content, after heating at 1500 ˚C under non-restrained conditions, the PLC increased as MgO content increased. On the other hand, the

PLCs of the restrained specimens were almost zero. This suggests that the restraint was effective. The APs of the test materials increased with increase in temperature as well as MgO content. While, the test materials heated under restrained conditions showed smaller APs.

The MORs increased as heating temperature rose. Restraint enhanced MOR increase after heating at 1500 ˚C. While a negative corelation was recognized between the MORs and the MgO content after heating without restraint, the MORs of all test materials after heating under restraint were equivalent. Similar tendancies for the MORs were recognizable for the dynamic MOEs after heating.

While influences of restraint were negligible for the test material containing 3 mass% of MgO, it became larger proportionally to the MgO content.

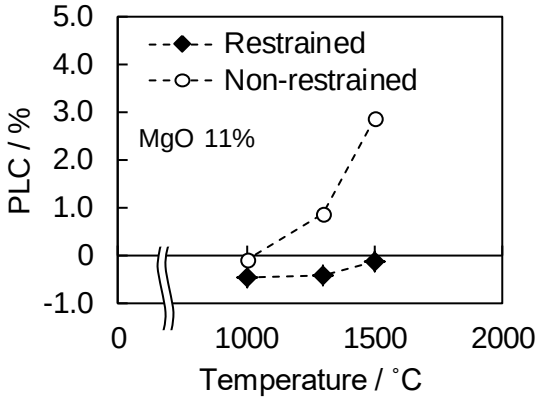

Figure 6. Permanent linear change of test material (a) after heating at various temperatures with and without restraint.

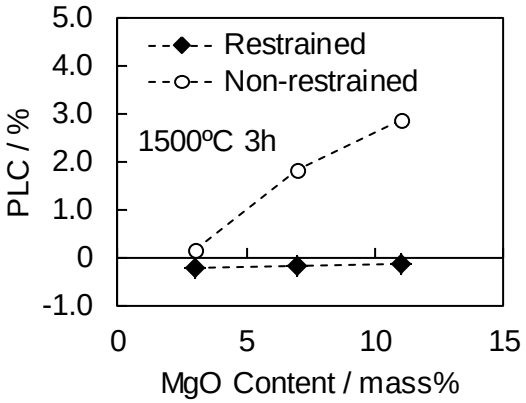

Figure 7. Variation in permanent linear change of test materials after heating at 1500 ˚C for 3 h with and without restraint as a function of MgO content.

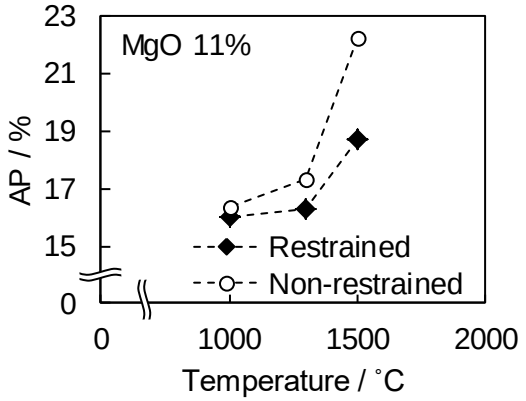

Figure 8. Apparent porosities of test material (a) after heating at various temperatures with and without restraint.

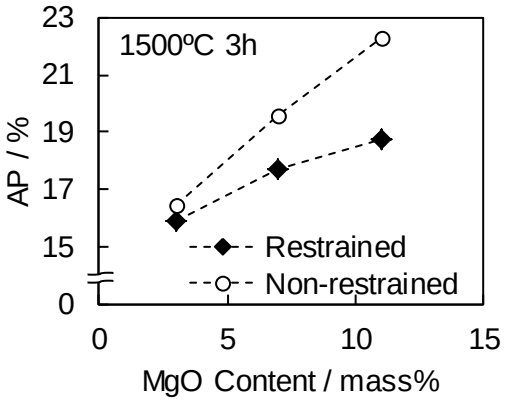

Figure 9. Variation in apparernt porosity of test materials after heating at 1500 ˚C for 3 h with and without restraint as a function of MgO content.

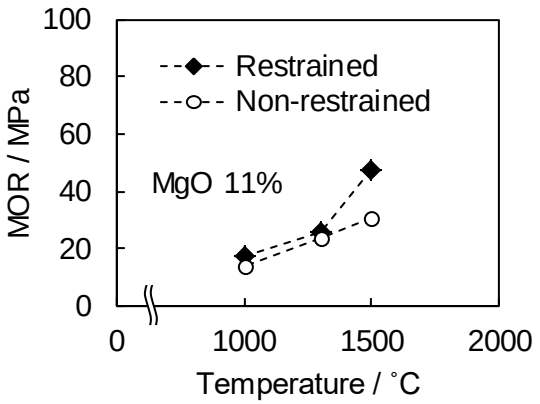

Figure 10. Modulus of ruptures of test material (a) after heating at various temperatures with and without restraint.

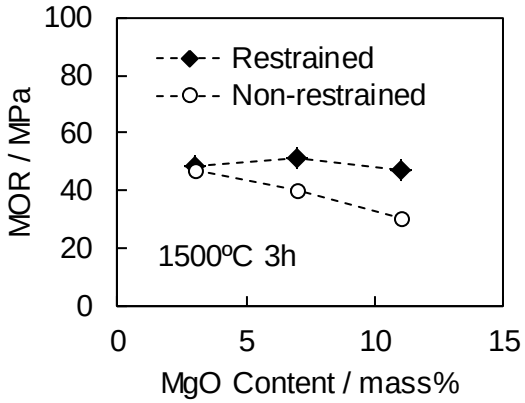

Figure 11. Variation in modulus of rupture of test materials after heating at 1500 ˚C for 3 h with and without restraint as a function of MgO content.

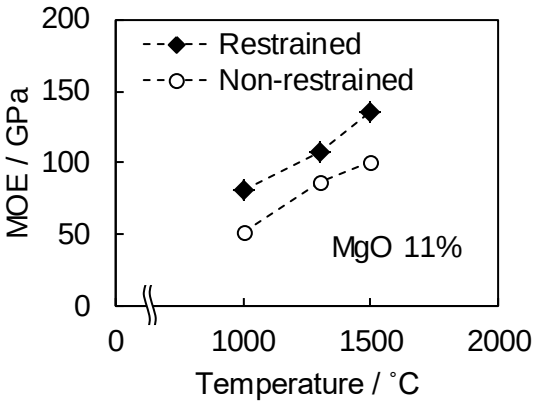

Figure 12. Dynamic Modulus of elasticity of test material (a) after heating at various temperatures with and without restraint.

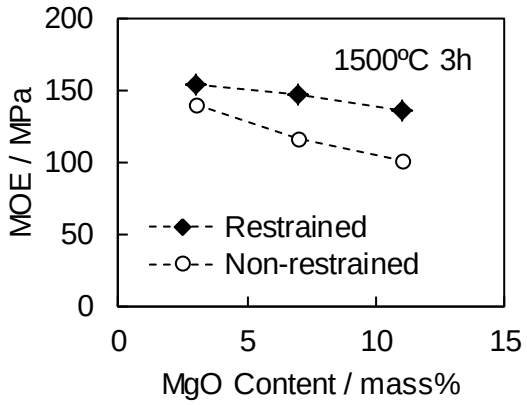

Figure 13. Variation in dynamic modulus of elasticity of test materials after heating at 1500 ˚C for 3 h with and without restraint as a function of MgO content.

Figures 14(A) and 14(B) show the compositional images of the test material (b) after being heated at 1500 ˚C without and with restraint, respectively. The images were taken perpendicular to the restraint plane (Figure 14(C)). In the images, the blackish areas indicate pores. As is obvious, smaller pores were observed for restrained specimens. It was quantified by pore size distribution as shown in Figure 15.

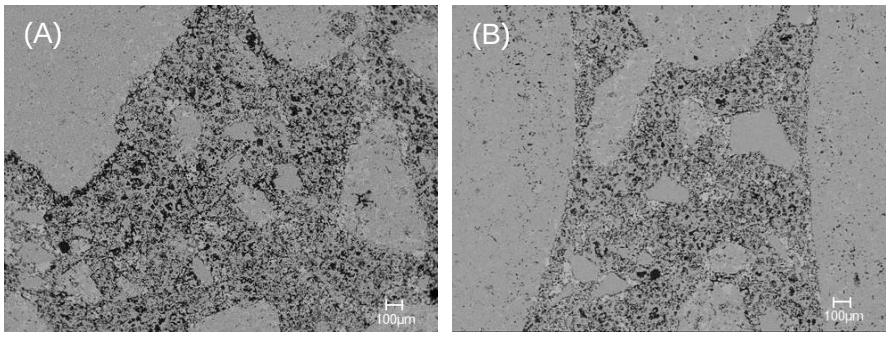

Figure 14. Microstructures of (A) non-restrained specimen and (B) restrained specimen.

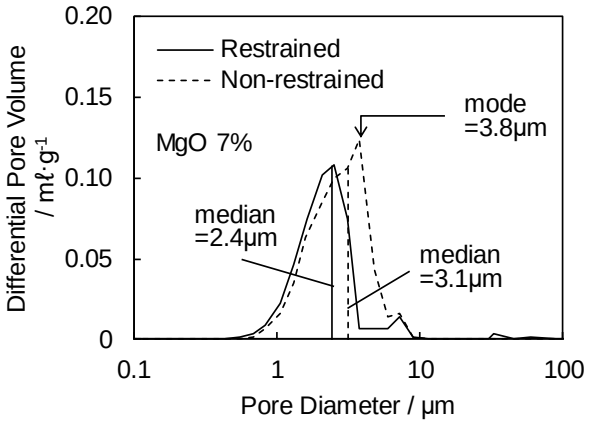

Figure 15. Pore-size distributions of restrained and non-restrained specimens after heating at 1500 ˚C.

3.3 Discussion

It is natural to hypothesize that variations in properties are attributable to microstructure evolution induced by an in-situ spinel forming reaction. Assuming that the densities of corundum (Al_2O_3), periclase (MgO) and spinel (Mg_2AlO_4) are 4000 kg/m^3, 3580 kg/m^3 and 3640 kg/m^3, respectively, 6.5 % increase in volume will accompany the spinel forming reaction. Thus, a 0.2 % increase in PLC is expected theoretically for the material containing 10 mol% of MgO. However, considerably larger PLCs were observed for test materials after heating at 1300 ˚C and 1500 ˚C without restraint. This disagreement is attributed to the reaction process in the test materials.

As described in PART I in this series of papers [7], the spinel forming reaction in alumina-magnesia refractories is caused by diffusion of Mg^{2+} through the liquid phase, which is formed along the rims of magnesia particles as a result of a eutectic melting reaction. Since spinel is a stable solid phase in the liquid, spinel precipitation and MgO dissolution continues until complete dissolution of MgO particles. In this process, spinel precipitates freely in the liquid phase to expand the inter-particle distances, resulting in rapid expansion as well as a larger PLC in comparison with the theoretical prediction. This results in large APs, which induce negative influence of MgO content on MORs and MOEs after heating at 1500 ˚C.

Although it is impossible to determine the rate controlling step of the reaction series in this study, all the reaction processes, i.e., eutectic melting, Mg^{2+} diffusion, spinel precipitation and MgO dissolution, would obey the Arrhenius equation. Thus, changing degrees of each property become larger with increase in temperature.

Inverse proportionality of the HMOE of test material (b) to temperature corresponds to the amount of liquid phase. Contrarily, the HMOE of the outer castable at 1300 ˚C was larger than that at 1000 ˚C. This is considered to be a result of the formation of a slight amount of liquid phase which connects particles tightly according to interfacial tension.

Under the restrained heating condition, it is impossible for the inter-particle distance to expand. Zero PLCs is evidence. Therefore, spinel tends to precipitate to fill the void among particles, resulting in lower APs and smaller pore sizes, in another word, densification. Improving effect of restraint on MORs and MOEs is attributed to densification.

Nevertheless, APs of test materials after heating at 1500 ˚C with restraint increased with the increase in MgO content. This suggests expansion in the direction perpendicular to the restrained plane. While no thickness measurement was carried out, 0.5 mm increase in thickness is expected for 2 % increase in AP.
In refractory linings of actual steel ladles, a difference in restraint stress along the lining thickness direction in accordance with temperature distribution is expected. Therefore, the difference in properties between the hot face and the back side is expected to be much larger than what has been predicted by heating experiments without restraint. This is an undesirable state in terms of structural spalling. In spite of the favorable influences of an in-situ spinel forming reaction in terms of corrosion resistance, the adverse effect on spalling resistance was clarified. Since the influence of restraint becomes larger with the increase in MgO content, careful attention should be paid for the determination of the MgO content of alumina-magnesia castables for steel ladles from the view point of spalling.

4 CONCLUSION

In order to reproduce the heating of alumina-magnesia castable refractories installed in actual steel ladles, heating experiments under restrained conditions were carried out for laboratorially prepared MgO content-varied test materials. Heating with restraint was achieved by heating the combined specimens of which high thermal expansion-alumina-magnesia castables were surrounded by low thermal expansion-alumina-silica castable. By using a simple mathematical model, restraint stresses were calculated to be in the range between 2 to 20 MPa, which are considered to be reasonable.
According to experimental results, it was found that restraint accelerates densification, which increases the modulus of elasticity and modulus of rupture of alumina-magnesia castables. Taking the temperature gradient found in an actual steel ladle lining into account, the difference in modulus of rupture and/or modulus of elasticity in the refractory lining was found to be much bigger than expected. This is an undesirable state in terms of spalling. These results are attributable to an in-situ spinel forming reaction that improves corrosion resistance. Since the difference in properties between the hot face and the back side is expected to be much larger than what has been predicted by heating experiments without restraint, careful attention is necessary to determine the MgO content of castables.

REFERENCES

1 Kobayashi M, Kataoka K, Sakamoto Y, Kifune I. Use of Alumina-Magnesia Castable in Steel Ladle Sidewalls. Taikabutsu Overseas. 1997; 17(3): 39-44.
2 Takakura Y, Yamamura T, Hamazaki Y, Kaneshige T. Thermal Characteristics of Alumina-Magnesia Castable. Taikabutsu. 1996; 48(9): 488-489.
3 Yamamoto K, Fujimoto H, Hanada F, Otani T, Hamazaki Y, Kaneshige T, Takakura Y. Application of Alumina-Magnesia Castable to Steel Ladle. Taikabutsu. 1996; 48(12): 656-657.
4 Ishikawa M, Takahashi N, Nishikawa C. Thermo-Mechanical Properties of Castable for Ladle Bottoms. Taikabutsu Overseas. 2000; 20(1): 28-31.
5 MAL Braulio, EY Sako, VC Pandolfelli. Expansion under Constraint and Its Effect on High-Alumina Spinel Forming Refractory Castables. Proceedings of the Unified International Technical Conference on Refractories (UNITECR 2013). 2013; 773-780.

6 Kitanaka M, Nishimura M, Nishida S. Effects of Coarse Aggregate on the Hot Properties of Castable Refractories. Taikabutsu Overseas. 2014; 34(2): 143.

7 Iida M, Doi N, Tomiya H, Torigoe A, Ramos VPS, Galesi DF, Leao CF. Technologies of Almina-Magnesia Refractories for Steel Ladles PART I, Brick Development. Associação Brasileira de Metalurgia, Materiais e Mineração. Proceedings of the 72th Annual Congress – International; 2017 October 2-6; PRO MAGNO, Brazil. São Paulo: ABM; 2017.